Journal of Visualized Experiments

# Fabrication of a strain measuring device with an improved 3D printer

--Manuscript Draft--

| | |
|---|---|
| **Article Type:** | Invited Methods Article - JoVE Produced Video |
| **Manuscript Number:** | JoVE60177R3 |
| **Full Title:** | Fabrication of a strain measuring device with an improved 3D printer |
| **Keywords:** | microscopic observation, amplifier, PDMS lens, strain measurement, 3D printing technology, spherical extrusion head |
| **Corresponding Author:** | Qiuyue Du<br>Beijing Technology and Business University<br>Beijing, Beijing CHINA |
| **Corresponding Author's Institution:** | Beijing Technology and Business University |
| **Corresponding Author E-Mail:** | duqiuyue@btbu.edu.cn |
| **Order of Authors:** | Qiuyue Du |
| | Weichao Wu |
| | Huiyu Xiang |
| **Additional Information:** | |
| **Question** | **Response** |
| Please indicate whether this article will be Standard Access or Open Access. | Standard Access (US$2,400) |
| Please indicate the **city, state/province, and country** where this article will be **filmed**. Please do not use abbreviations. | Beijing |

Dear Editor,

Attached please find the word version of my paper entitled " Fabrication of Strain measuring device based on improved 3D printer" with the kind request to consider it for publication in the journal of visualized experiments. We hope that it will be published in January 2020.

The authors claim that none of the material in the paper has been published or is under consideration for publication elsewhere. Should you receive the paper, please send me an e-mail to confirm receipt of it.

Thanks a lot in advance!

Best regards,

Qiuyue Du

**TITLE:**

# Production of a Strain-Measuring Device with an Improved 3D Printer

**AUTHORS AND AFFILIATIONS:**

Qiuyue Du, Weichao Wu, Huiyu Xiang

Department of Materials Science and Mechanical Engineering, Beijing Technology and Business University, Beijing, China

**Corresponding Author:**

Qiuyue Du (duqiuyue@btbu.edu.cn)

**Email Addresses of Co-authors:**

Weichao Wu (13146917900@163.com)

Huiyu Xiang (xianghy@th.btbu.edu.cn)

**KEYWORDS:**

microscopic observation, amplifier, PDMS lens, strain measurement, 3D printing technology, spherical extrusion head

**SUMMARY:**

This work presents a strain measurement sensor consisting of an amplification mechanism and a polydimethylsiloxane microscope manufactured using an improved 3D printer.

**ABSTRACT:**

A traditional strain measurement sensor needs to be electrified and is susceptible to electromagnetic interference. In order to solve the fluctuations in the analog electrical signal in a traditional strain gauge operation, a new strain measurement method is presented here. It uses a photographic technique to display the strain change by amplifying the change of the pointer displacement of the mechanism. A visual polydimethylsiloxane (PDMS) lens with a focal length of 7.16 mm was added to a smartphone camera to generate a lens group acting as a microscope to capture images. It had an equivalent focal length of 5.74 mm. Acrylonitrile butadiene styrene (ABS) and nylon amplifiers were used to test the influence of different materials on the sensor performance. The production of the amplifiers and PDMS lens is based on improved 3D printing technology. The data obtained were compared with the results from finite element analysis (FEA) to verify their validity. The sensitivity of the ABS amplifier was 36.03 ± 1.34 με/μm, and the sensitivity of the nylon amplifier was 36.55 ± 0.53 με/μm.

**INTRODUCTION:**

Obtaining light but strong materials is particularly important in modern industry. The properties of materials are affected when subjected to stress, pressure, torsion, and bending vibration during use[1,2]. Thus, strain measurement of materials is important to analyze their durability and troubleshoot usage. Such measurements enable engineers to analyze the durability of materials and troubleshoot production problems. The most common strain measurement method in

industry uses strain sensors[3]. Traditional foil sensors are widely used because of their low cost and good reliability[4]. They measure the changes in electrical signals and convert them to different output signals[5,6]. However, this method leaves out the details of the strain profile in the measured object and is susceptible to noise from vibrational electromagnetic interference with analog signals. Developing accurate, highly repeatable, and easy material strain measurement methods is important in engineering. Thus, other methods are being studied.

In recent years, nanomaterials have drawn much interest from investigators. To measure strain on small objects, Osborn et al.[7,8] proposed a method to measure the strain of 3D nanomaterials using electron backscatter (EBSD). Using molecular dynamics, Lina et al.[9] investigated the interlayer friction strain engineering of graphene. Distributed optical fiber strain measurements using Rayleigh backscatter spectroscopy (RBS) have been widely used in fault detection and for the evaluation of optical devices due to their high spatial resolution and sensitivity[10]. Grating fiber optic (FBG)[11,12] distributed strain sensors have been widely used for high-precision strain measurement[13] for their sensitivity to temperature and strain. In order to monitor the strain changes caused by curing after resin injection, Sanchez et al.[14] embedded a fiberoptic sensor into an epoxy carbon fiber plate and measured the complete strain process. Differential interference contrast (DIC) is a powerful measurement method of the field deformation[15-17] that is widely used as well[18]. By comparing the changes of measured surface gray levels in the collected images, the deformation is analyzed, and the strain calculated. Zhang et al.[19] proposed a method that relies on the introduction of reinforced particles and DIC images to evolve from traditional DIC. Vogel and Lee[20] calculated strain values using an automatic two-view method. In recent years, this enabled simultaneous microstructure observation and strain measurement in particle-reinforced composites. Traditional strain sensors only effectively measure strain in one direction. Zymelka et al.[21] proposed an omnidirectional flexible strain sensor that improves a traditional strain gauge method by detecting changes in the sensor resistance. It is also possible to measure strain using biological or chemical substances. For instance, ionic conductive hydrogels are an effective alternative to strain/tactile sensors due to their good tensile properties and high sensitivity[22,23]. Graphene and its composites have excellent mechanical properties and provide a high carrier mobility along with good piezoresistivity[24-26]. Consequently, graphene-based strain sensors have been widely used in electronic skin health monitoring, wearable electronics, and other fields[27,28].

In this work, a conceptual strain measurement using a polydimethylsiloxane (PDMS) microscope and an amplification system is presented. The device is different from a traditional strain gauge because it does not require wires or electrical connections. Moreover, displacement can be observed directly. The amplification mechanism can be placed at any location on the tested object, which greatly increases the repeatability of the measurements. In this study, a sensor and a strain amplifier were made by 3D printing technology. We first improved the 3D printer to increase its efficiency for our requirements. A spherical extrusion device was designed to replace the traditional single-material extruder controlled by the slicing software to complete the conversion of the metal and plastic nozzles. The corresponding molding platform was changed, and the displacement-sensing device (amplifier) and the reading device (PDMS microscope) were integrated.

**PROTOCOL:**

**1. Assembly of the amplification mechanism**

1.1. Construct an experimental platform including an improved 3D printer, a strain gauge indicator, a driving device, a support frame, an aluminum bar, a PDMS lens, a smartphone, weights, a printed amplifier (**Supplemental Figure 1**), and a strain gauge, as shown in **Figure 1**.

1.2. Set the height of each layer in the printer at 0.05 mm for nylon and 0.2 mm for ABS. Set the diameter of the printing head to 0.2 mm in both cases. Set the temperature of the nozzle to 220 °C for nylon and 100 °C for ABS. Finally, set the printing speed to 2,000 mm/min for nylon and 3,500 mm/min for ABS.

1.3. Adjust the orientation of the spherical extrusion head so that the metal nozzle faces the low-temperature platform and print a contour to ensure a normal extrusion, as shown in **Figure 2**.

1.4. Hang the nylon and ABS on the column. The front end must enter the printing coil container to be melted by the metal nozzle.

**2. Assembly of the PDMS microscope**

2.1. Using a magnetic stirrer, mix the PDMS precursor and the curing agent to obtain a weight ratio of 10:1.

2.2. Place the mixture into the degasser for 40 min to remove bubbles and pour the degassed mixture into the PDMS container of the spherical extrusion head.

2.3. Rotate the spherical extrusion head and the platform so that the plastic nozzle faces the high-temperature platform.

2.4. Set the plastic nozzle increment to 50 µL. Place the bottom end of the pipette device 20 mm[29] away from the mold by using the nozzle rotation and the stepper motor in the Z-axis.

2.5. Turn on the hot plate to heat the high-temperature platform. The temperature of the platform is controlled by a non-contact infrared radiation thermometer.

NOTE: This study tested temperatures of 140 °C, 160 °C, 180 °C, 200 °C, 220 °C, and 240 °C.

2.6. Squeeze the PDMS container to print the PDMS lens.

2.7. Cool the PDMS lens to room temperature and remove it with rubber tweezers.

2.8. Determine the geometrical parameters of the lens, including the contact angle, the curvature radius, and the droplet diameter, using a three-dimensional shape analyzer.

## 3. Strain measurement for loading tests in the control and test groups

3.1. Use a bar made of aluminum 6063 T83 as the cantilever beam. The length, width, and thickness of the cantilever beam should be 380 mm x 51 mm x 3.8 mm, respectively. Fix one end to the operating table with bolts and nuts.

3.2. Draw a cross at the center and 160 mm from the free end of the cantilever beam.

3.3. To remove the oxide layer on the cantilever beam, polish its surface with fine sandpaper before pasting. The grinding direction should be about 45° from the direction of the strain gauge wire grid. Use cotton wool soaked in acetone to wipe the surface of the cantilever beam and the surface of the strain gauge paste.

3.4. Connect the driving device and the strain gauge indicator. Turn on the power. Use a strain gauge mounted onto the center surface of the aluminum bar at its fixed end to measure the strain changes.

3.5. Fix the standard weight to the free end of the cantilever beam to control the concentrated force input. Read the data using a conventional strain gauge indicator with a quarter-bridge connection method.

3.6. Replace the strain gauge with the ABS and nylon amplifiers at the same location.

3.7. Attach the PDMS lens onto the smartphone camera with an 8-megapixel sensor at a focus distance of 29 mm. Adjust the focal length of the camera until a clear image is obtained. Read the displacement of the pointer using the PDMS microscope.

3.8. Repeat steps 3.5 and 3.6, setting the load to 1 N, 2 N, 3 N, 4 N, and 5 N each time.

## 4. Finite element analysis

4.1. Establish 3D finite element models of the nylon and ABS parts for strain measurement (see **Table of Materials** for software used). Import the cantilever beam and the amplifying mechanism into the material library of the software and simulate their placement positions.

4.2. Analyze the mechanical properties of the amplifying mechanism pointer under the action of a cantilever beam.

4.3. Generate meshes for use in 3D geometric models using tetrahedral elements with a fine element size. Refine the flexure hinges, especially the hinge between the pointer and the other bodies.

NOTE: The Young moduli of elasticity used for aluminum, nylon, and ABS were 69 GPa, 2 GPa,

and 2.3 GPa, respectively. The Poisson ratios used for aluminum, nylon, and ABS were 0.33, 0.44, and 0.394, respectively.

4.4. Apply a concentrated force of 1 N to the center of the free end of the cantilever beam. Repeat with 2 N, 3 N, 4 N, and 5 N.

**REPRESENTATIVE RESULTS:**

When the platform temperature increased, the droplet diameter and the curvature radius decreased, whereas the contact angle increased (**Figure 3**). Therefore, the focal length of the PDMS increased. However, for platform temperatures above 220 °C, a very short curing time was observed in the droplets, and they could not extend into a plane-convex shape. This can be attributed to the low attachment area when adhering onto a smartphone camera. Therefore, only soft lenses formed at 220 °C were used as magnifiers in all tests. The focal length of the PDMS lens was 7.16 mm for an optical power of 140 $m^{-1}$. The droplet diameter was 2.831 mm and the maximum cone angle was 46.68°, which yielded a numerical aperture (NA) of about 0.40, close to a 20x magnification. The focal length of the lens group can be calculated as $f_1 \times f_2 / (f_1 + f_2 - s)$, where $f_1$ is the focal length of the PDMS lens, $f_2$ is the focal length of the camera lens, and $s$ is the distance between them. Assuming $s$ = 0, the effective focusing distance of the PDMS microscope was 5.74 mm.

The calibration between the control group and the test group was done using the measurement sensitivity $K$, expressed as $K = \varepsilon/\Delta l_p$, where $\varepsilon$ is the strain obtained by the strain indicator and $\Delta l_p$ is the output of the pointer. **Figure 4A** shows the comparison of the experimental displacement measurement with the FEA simulations for nylon. The experimental and FEA slopes varied from 0.027−0.097 (2.74%−9.36%). **Figure 4B** shows the minimum and maximum discrepancies between the slopes for ABS of 0.026 and 0.07 (3.85% and 9.94%). **Figure 5** shows $K$ for nylon and ABS. The study found that $K_{nylon} = 36.55 \pm 0.53$ με/μm and $K_{ABS} = 36.03 \pm 1.34$ με/μm.

**FIGURE AND TABLE LEGENDS:**

**Figure 1. Experimental test setup, including the improved 3D printer, a strain gauge indicator, a driving device, a support frame, an aluminum bar, a PDMS lens, a smartphone, weights, a printed amplifier, and a strain gauge.**

**Figure 2. Details of the two-phase solid-liquid 3D printer.**

**Figure 3. Droplet diameter, curvature radius, and contact angle of the PDMS lens at different temperatures.**

**Figure 4. Relations between the displacement of the pointer and the different concentrated forces for nylon and ABS, respectively.** With the same parameters of the improved 3D printer, five nylon amplifiers (a–e) and five ABS amplifiers (a–e) were printed. The test for each group was repeated ten times.

**Figure 5. Correlation between the displacement and the strain for nylon and ABS.** The letters

a–e represent the five samples for each material. The sensitivity *K* of nylon and of ABS was obtained by averaging the five slopes.

**DISCUSSION:**

The output displacement evolved linearly with the force concentrated at the free end of the cantilever beam and was consistent with the FEA simulations. The sensitivity of the amplifiers was 36.55 ± 0.53 με/μm for nylon and 36.03 ± 1.34 με/μm for ABS. The stable sensitivity confirmed the feasibility and the effectiveness of the rapid prototyping of high-precision sensors using 3D printing. The amplifiers had a high sensitivity and were free of electromagnetic interference. In addition, they had a simple structure, a small volume, and a low weight. Different materials must be set differently in the printing process based on multiple variables, including the layer thickness, the nozzle diameter, and the feed rate. The specific values need to be combined with different printer parameters and are determined after repeated debugging steps. This flexible manufacturing method enables changing the material and the size instantly according to the actual working conditions. This can increase the performance by adding electrical insulation and making it explosion-proof. It enables the miniaturization, the customized production, and the use of high-precision displacement sensors.

To obtain a 5.74 mm macro shot, the lens group consisted of a PDMS lens and a smartphone camera. The basic parameters affecting the optical quality of the PDMS lens formation, including the contact surface diameter, the radius of curvature, and the contact angle, were determined by the temperature of the production platform and the solution volume for a constant drop height. The temperature was precisely controlled by a hot plate and noncontact infrared thermometers. The solution volume was 50 μL per drop through the plastic nozzle. The camera needed to be wiped with alcohol to remove impurities like dust to ensure that the PDMS lens adhered closely to increase the combined time and the sharpness. By adjusting the parameters of the instruments and the solutions used, the system can be adapted for various noncontact micromeasurements in various fields.

The rapid manufacturing of the sensor was achieved using the two-cavity structure of the spherical extrusion head and the one-machine formation of a two-phase solid-liquid material. The printing coil container was used to introduce a solid wire, and the amplifier was printed by hot melting of the metal nozzle. The PDMS container was made of a soft material and contained a mixed PDMS solution. The solution was precisely squeezed out from the plastic nozzle. This technology can also be applied to the manufacturing of structural microsphere materials in various fields, including electronics, biopharmaceuticals, energy, and defense sectors.

This work demonstrated a real-time strain measurement system with an amplifier, a PDMS lens, and a smartphone that can replace the traditional complex strain gauge-strain gauge-bridge test method. In addition, a two-phase solid-liquid 3D printer with high precision, low cost, and a rapid repetitive production is shown. During solid printing, the thickness of the nylon layer was set to 0.05 mm, the nozzle temperature was 220 °C, the printing speed was 2,000 mm/min. The thickness of the ABS layer was 0.2 mm, the nozzle temperature was 100 °C, and the printing speed was 3,500 mm/min. The printing parameters need to be combined with the inherent

material melting speed, temperature, and viscoelasticity to obtain the best printing performance; the printer layer accuracy, feed range, and printing speed need to be considered as well. During liquid printing, the PDMS needed to have a weight ratio of 10:1 of precursor solution and curing agent and the hanging drop height was fixed to 20 mm, which controlled the molding rate of the lens for 60 s. The high-temperature platform was made of glass and its temperature was controlled by a hot plate and a noncontact infrared radiation thermometer. The geometric parameters of the lens varied greatly with the surface temperatures tested (140 °C, 160 °C, 180 °C, 200 °C, 220 °C, and 240 °C). The optical properties of the PDMS lens molded at 220 °C with 50 µL of solution produced the best results in the measurement system designed. It is possible to manufacture individualized lenses with different optical properties and sizes by adjusting the solution ratio, the volume, the molding temperature, and the hanging height. The wide range of applications related to microstructure deformation that can be measured by this method is bound to increase.

**ACKNOWLEDGMENTS:**

This work was financially supported by the National Science Foundation of China (Grant No. 51805009).

**DISCLOSURES:**

The authors declare no conflicting interests.

**REFERENCES:**

1**.** Laramore, D., Walter, W., Bahadori, A. Design of a micro-nuclear-mechanical system for strain measurement. *Radiation Physics and Chemistry*. **155** (8), 209−212 (2019).

2. Hu, D., Song, B., Dang, L., Zhang, Z. Effect of strain rate on mechanical properties of the bamboo material under quasi-static and dynamic loading condition. *Composite Structures*. **200** (4), 635−646 (2018).

3. Mattana, G., Briand, D. Recent advances in printed sensors on foil. *Materials Today*. **19** (2), 88−99 (2016).

4. Laramore, D., McNeil, W., Bahadori, A. A. Design of a micro-nuclear-mechanical system for strain measurement. *Radiation Physics and Chemistry*. **281**, 258−263 (2018).

5. Enser, H., Sell, J. K., Hilber, W., Jakoby, B. Printed strain sensors in organic coatings: In depth analysis of sensor signal effects. *Sensors and Actuators A: Physical*. **19** (2), 88−99 (2016).

6. Kelb, C., Reithmeier, E., Roth, B. Foil-integrated 2D Optical Strain Sensors. *Procedia Technology*. **15**, 710−715 (2014).

7. Osborn, W., Friedman, L. H., Vaudin, M. Strain measurement of 3D structured nanodevices by EBSD. *Ultramicroscopy*. **184**, 88−83 (2018).

8. Liu, F., Guo, C., Xin, R., Wu, G., Liu, Q. Evaluation of the reliability of twin variant analysis in Mg alloys by in situ EBSD technique. *Journal of Magnesium and Alloys*. **150** (4), 184−198.

9. Lin, X., Zhang, H., Guo, Z., Chang, T. Strain engineering of friction between graphene layers. *Journal of Tribology International*. **131** (8), 686–693 (2019).

10. Shingo, O. Long-range measurement of Rayleigh scatter signature beyond laser coherence length based on coherent optical frequency domain reflectometry. *Journal of Optics Express*. **24** (17), 19651 (2016).

11. Davis, C., Tejedor, S., Grabovac, I., Kopczyk, J., Nuyens, T. High-Strain Fiber Bragg Gratings for Structural Fatigue Testing of Military Aircraft. *Journal of Photonic Sensors*. **2** (3), 215−224 (2012).
12. Peng, J., Jia, S., Jin, Y., Xu, S., Xu, Z. Design and investigation of a sensitivity-enhanced fiber Bragg Grating sensor for micro-strain measurement. *Journal of Sensors and Actuators*. **285**, 437−447 (2019).
13. Hong, C. Y., Zhang, Y. F., Yang, Y. Y., Yuan, Y. An FBG based displacement transducer for small soil deformation measurement. *Sensors and Actuators A: Physical*. **286**, 35−42 (2019).
14. Sánchez, D. Z., Gresil, M., Soutis, C. Distributed internal strain measurement during composite manufacturing using optical fibre sensors. *Composites Science and Technology*. **120**, 49−57 (2015).
15. Castillo, D. R., Allen, T., Henry, R., Giffith, M., Ingham, J. Digital image correlation (DIC) for measurement of strains and displacements in coarse, low volume-fraction FRP composites used in civil infrastructure. *Composite Structures*. **212** (10), 43−57 (2019).
16. Badadani, V., Sriranga, T. S., Srivatsa, S. R. Analysis of Uncertainty in Digital Image Correlation Technique for Strain Measurement. *Materials Today: Proceedings*. **5** (10), 20912 20919 (2018).
17. Gao, C., Zhang, Z., Amirmaleki, M., Tam, J., Sun, Y. Local strain mapping of GO nanosheets under in situ TEM tensile testing. *Applied Materials Today*. **14**, 102−107 (2018).
18. Chine, C. H., Su, T. H., Huang, C. J., Chao, Y. J. Application of digital image correlation (DIC) to sloshing liquids. *Optics and Lasers in Engineering*. **115**, 42−52 (2019).
19. Zhang, F., Chen, Z., Zhong, S., Chen H., Wang, H. W. Strain measurement of particle reinforced composites at microscale: an approach towards concurrent characterization of strain and microstructure. *Micron*. (2019).
20. Vogel, J. H., Lee, D. An automated two-view method for determining strain distributions on deformed surfaces. *Journal of Materials Shaping Technology*. **6** (4), 205–216 (1988).
21. Zymelka, D., Yamashita, T., Takamatsu, S., Kobayashi, T. Thin-film flexible sensor for omnidirectional strain measurements. *Journal of Sensors and Actuators*. **263**, 391−397 (2017).
22. Li, R., Zhang, K., Cai, L., Chen, G., He, M. Highly stretchable ionic conducting hydrogels for strain/tactile sensors. *Polymer*. **167** (12), 154−158 (2019).
23. Liu, H., Macqueen, L. A., Usprech, J. F, Maleki, H. Microdevice arrays with strain sensors for 3D mechanical stimulation and monitoring of engineered tissues. *Biomaterials*. **172**, 30−40 (2018).
24. Bolotin, K. I., Sikes, K. J., Jiang, Z., Stormer, H. L. Ultrahigh electron mobility in suspended Graphene. *Solid State Communications.* **146** (9–10), 351–355 (2008).
25. Smith, A. D., et al. Electromechanical piezoresistive sensing in suspended graphene membranes. *Nano Letters*. **13** (7), 3237–3242 (2013).
26. Zhao, J., Wang, G., Yang, R., Lu, X., Cheng, M. Tunable piezoresistivity of nanographene films for strain sensing. *ACS Nano*. **9** (2), 1622–1629 (2015).
27. Bae, S.H., Lee, Y. B., Sharma, B. K. Graphene-based transparent strain sensor. *Carbon*. **51,** 236–242 (2013).
28. Boland, C.S, Khan U. Sensitive electromechanical sensors using viscoelastic graphene polymer nanocomposites. *Science*. **354** (6317), 1257–1260 (2016).
29. Sung, Y. L, Jeang J., Lee, C. H., Shih, W. C. Fabricating optical lenses by inkjet printing and

353 heat-assisted in situ curing of polydimethylsiloxane for smartphone microscopy. *Journal of*
354 *Biomedical Optics*. **20** (4), 047005 (2015).

Figure1

Click here to access/download;Figure;FIG 1.ai

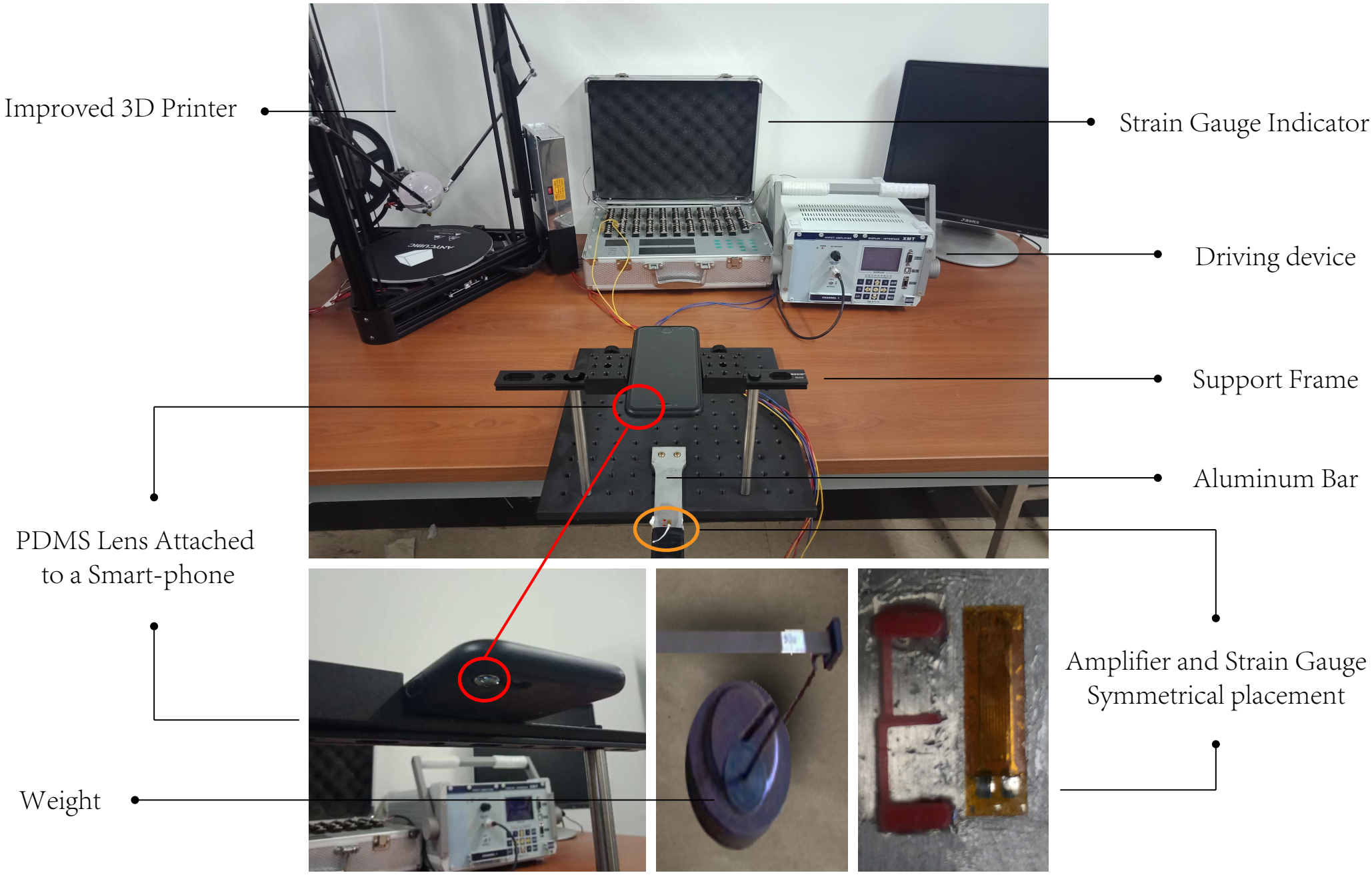

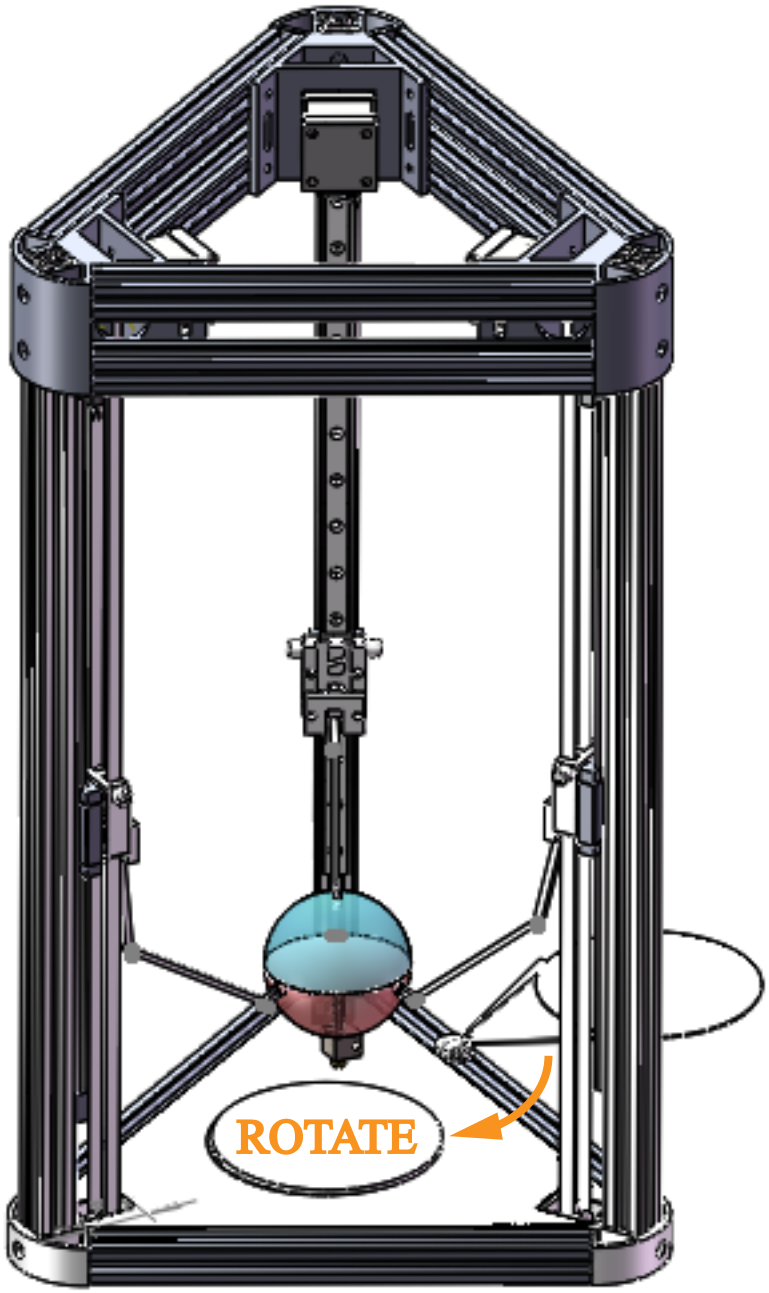


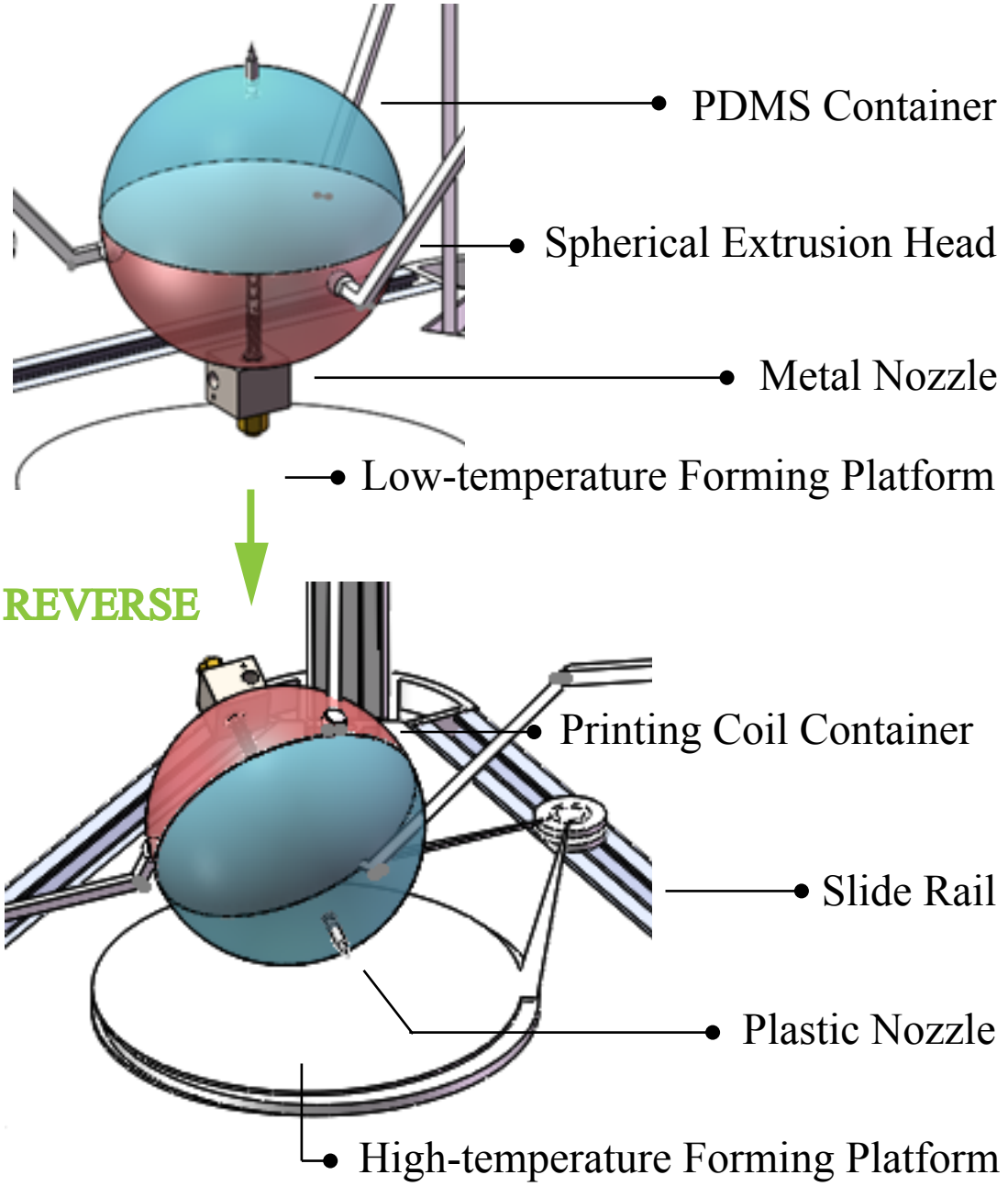

Figure3

Click here to access/download;Figure;FIG 3.ai

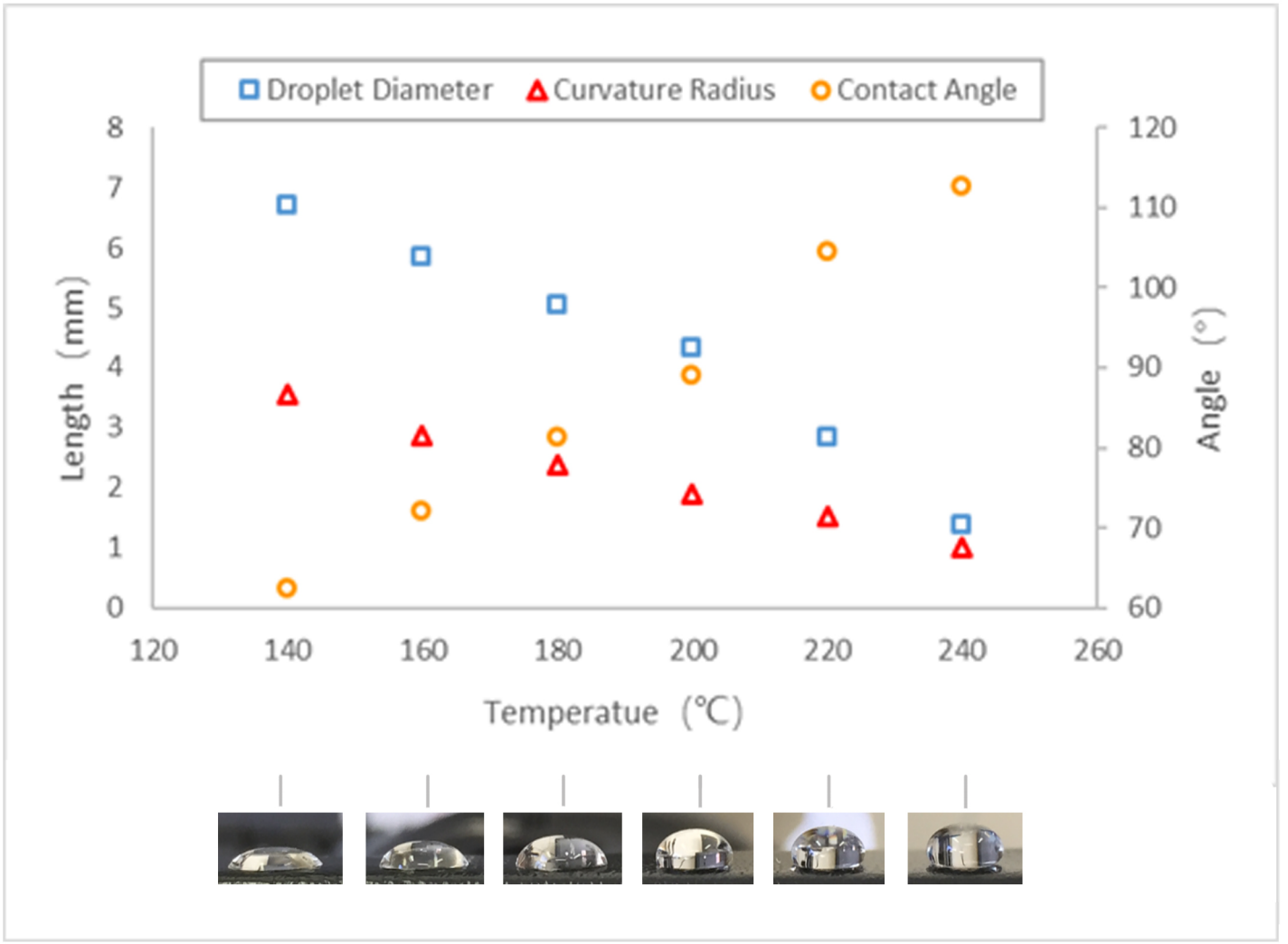

Figure4

Click here to access/download;Figure;FIG 4.ai

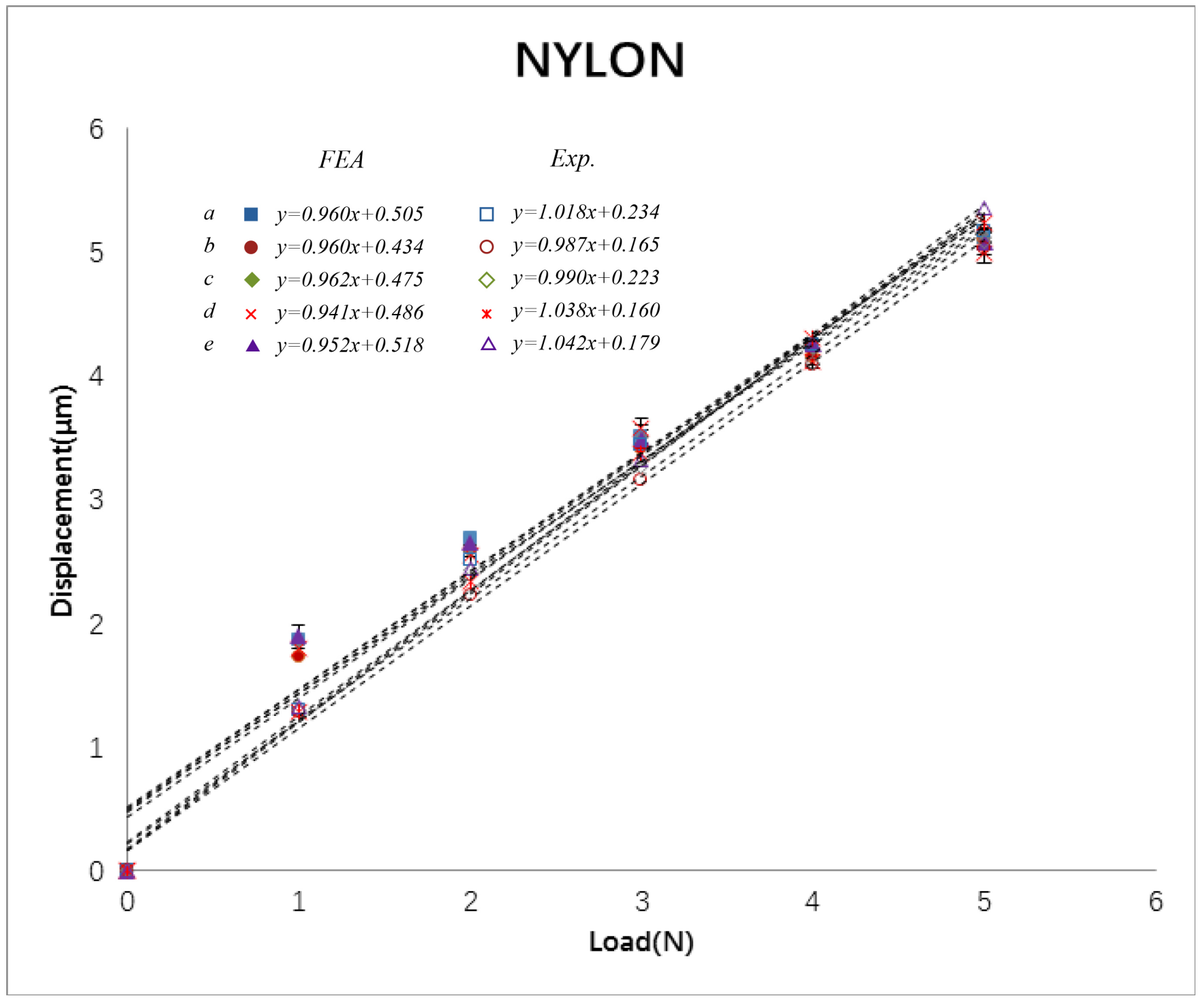


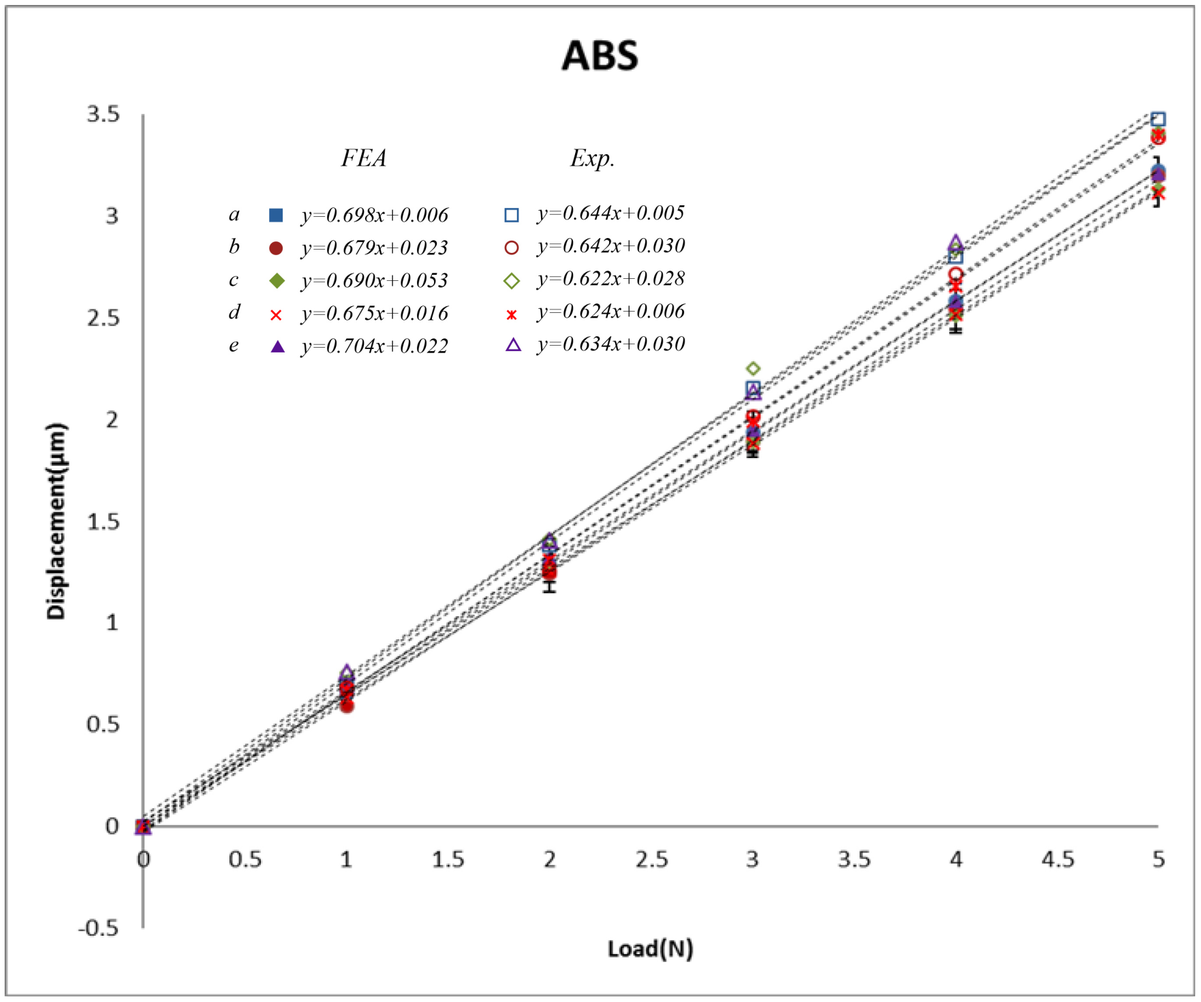

Figure5

Click here to access/download;Figure;FIG 5.ai

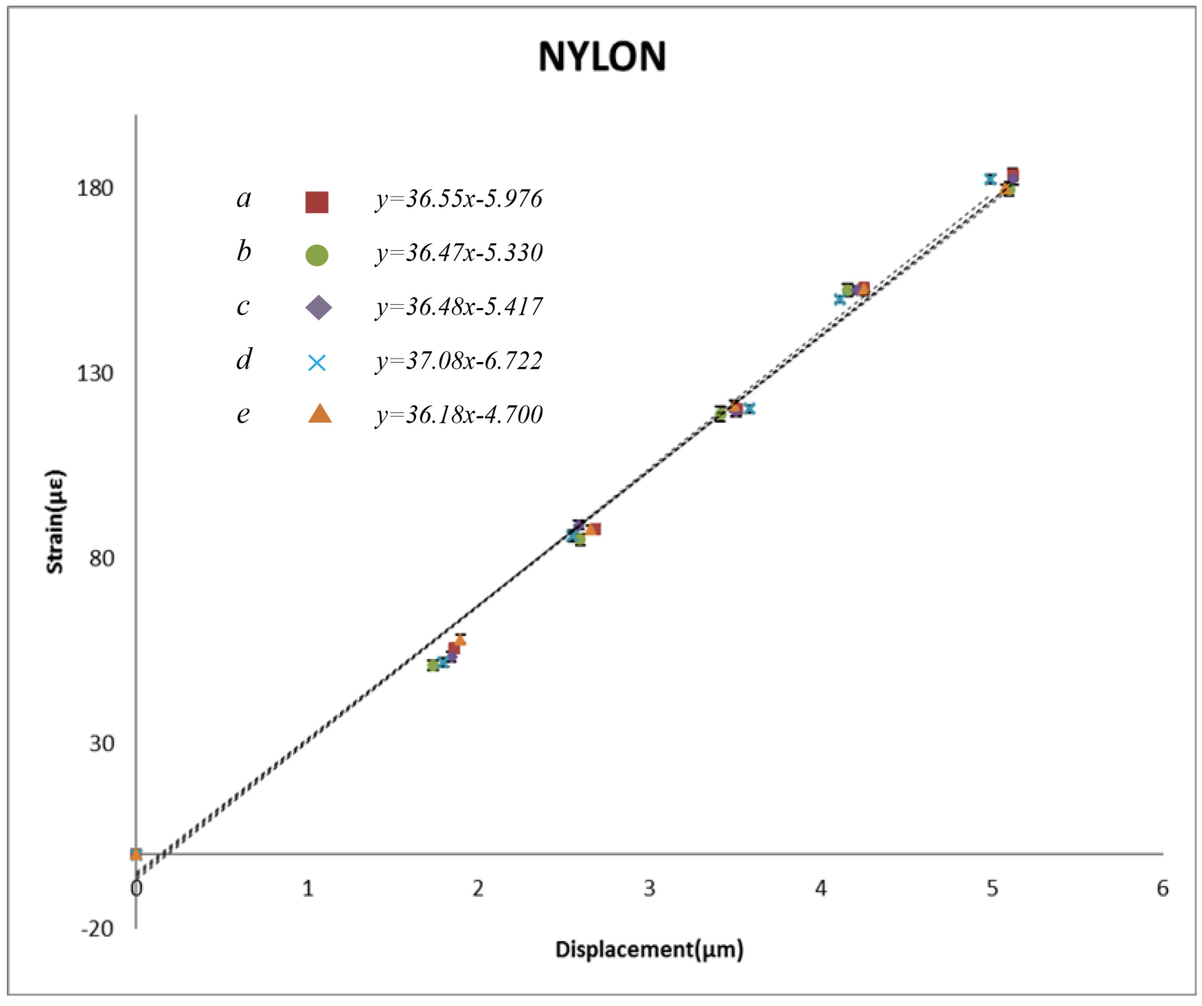


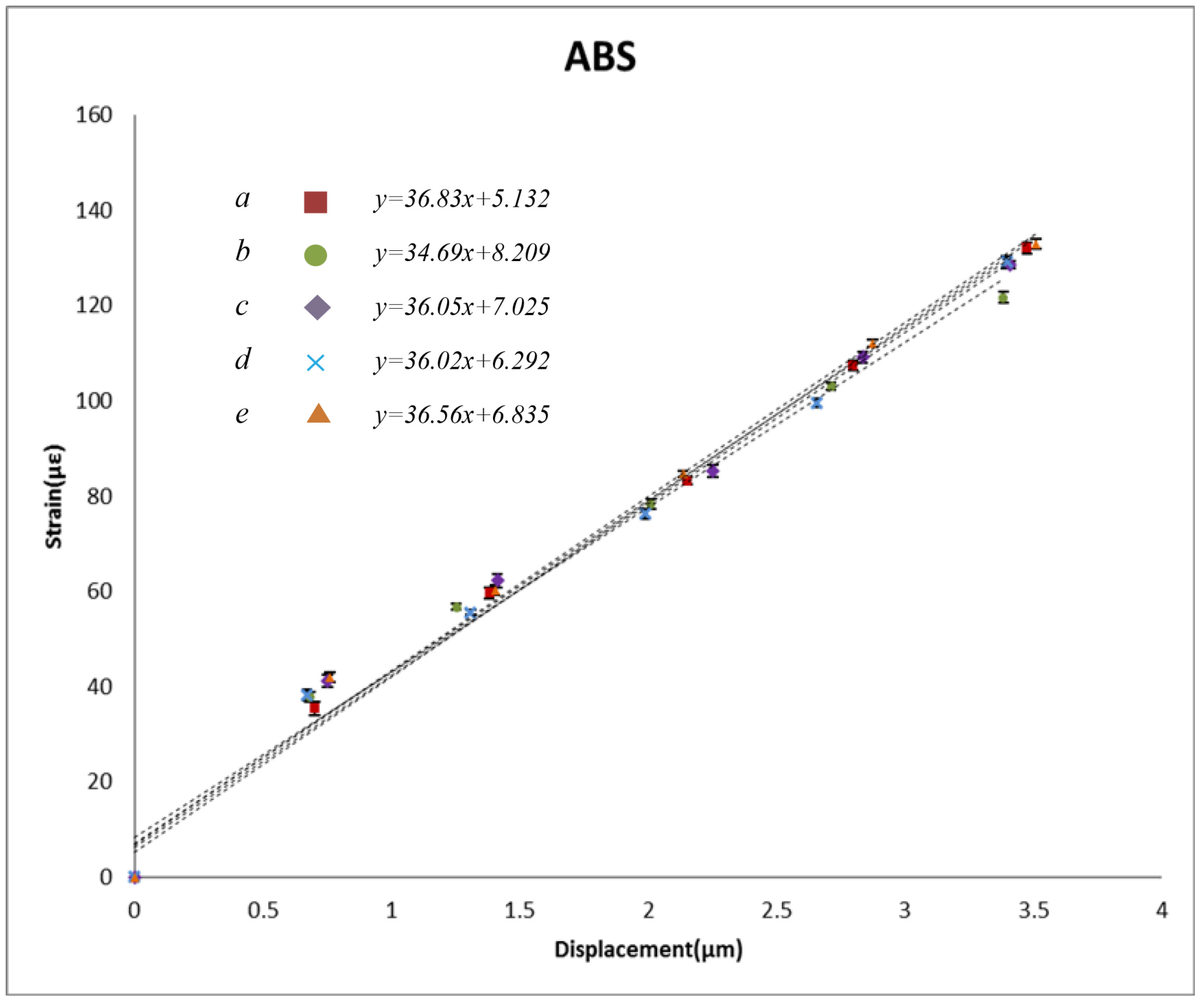

| Name of Material/Equipment | Company | Catalog Number | Comments/Description |
|---|---|---|---|
| ABS | Hengli dejian plastic electrical products factory | | Used for printing 1.75 mm diameter wire for am |
| Aluminum 6063 T83 bar | | | The length, width and thickness of cantilever bea |
| ANSYS | ANSYS | ANSYS 14.5 | |
| CURA | Ultimaker | Cura 3.0 | Slicing softare,using with the improved 3D printe |
| Curing agent | Dow Corning | | PDMS and curing agent are mixed with the weigl |
| Driving device | Xinmingtian | E00 | |
| Improved 3D printer and accessories | | | Made by myself. The rotary spherical lifting platf |
| iPhone 6 | Apple | MG4A2CH/A | 8-megapixel sensor and the equivalent focus dis |
| Magenetic stirrer | SCILOGEX | MS-H280-Pro | |
| Nylon | Hengli dejian plastic electrical products factory | | Used for printing 1.75 mm diameter wire for am |
| PDMS | Dow Corning | SYLGARDDC184 | After the viscous mixture is heated and hardene |
| Shape analyzer | Gltech | SURFIEW 4000 | |
| Solidworks | Dassault Systems | Solidworks 2017 | Assist to modelling |
| VISHAY strain gauge | Vishay | | Used to measure the strain produced in the expe |
| VISHAY strain gauge indicator | Vishay | | Strain data acquisition. |

plifying mechanism
am are 380 mm, 51 mm, and 3.8 mm.

er
ht ratio of 10:1

orm is adopted. The spherical lifting platform is equipped with a nozzle and a pipette, which can be switched and printed freely. With a ro
tance is 29mm

plifying mechanism
d, it can be combined with the lens amplification device of the mobile phone for image acquisition.

eriment.

ɔtary printing platform, the platform temperature can be freely controlled.

Author License Agreement (ALA)

Click here to access/download;Author License Agreement (ALA);Agreement.jpg

Dear Editor:

Thank you for your letter concerning our manuscript entitled “Fabrication of a strain measuring device with an improved 3D printer” (ID: JoVE60177). The comments were valuable and very helpful to improve our manuscript. We have made corrections that will answer your requests. The revised portions are marked in red in the revised manuscript. Please find here the detailed answers to your correction request.

1. Figures 4-5: The figure legends here are still unclear. Even if you were to remove a-e, there are still 10 (Figure 4 A and B) or 5 (Figure 5 A and B) different data sets in each figure, which are not explained anywhere. Is each dataset a different experiment? Do, e.g., the filled and open blue squares (‘a’ dataset) have anything to do with each other? It would appear not, in which case it appears that, e.g., the maximum difference between FEA and experimental slopes for nylon would be 0.101 (FEA red x and Exp. open purple triangle). Please explain your figures more thoroughly in the legends and double-check these results.

Response: Legends for Figure 4 and Figure 5 have been rewritten to make them clearer. Figure 4: Relations between the displacement of the pointer and the different concentrated forces for nylon and ABS, respectively. With the same parameters of the improved 3D printer, we have printed five nylon amplifiers (numbers from a to e) and five ABS amplifiers (numbers from a to e). As shown in Figure 4a, group “a” illustrates the mean result of FEA and experimental test for “amplifier a” for nylon, and other groups show that of the amplifier b, c, d, e. Test for each group has been repeated for ten times. Figure 5: Correlation between the displacement and the strain for nylon and ABS, respectively. Letters a-e represent the five samples for each material. The sensitivity $K$ of nylon is obtained by averaging the five slopes, as well as ABS.

Five samples were made from each material, and each sample was measured ten times. Although there are some deviations between the ideal value (FEA) and the actual results (experimental test) for one sample, and size deviation between the five samples, the experimental results are linear, which proves the feasibility and validity of the proposed sensor. Future work will further explore various factors affecting the sensitivity of the proposed sensor system, and improve the operating accuracy of the improved 3D printer.

2. Protocol step 1.1: 'Figure 1' here still seems to refer to supplemental Figure 1, which contains the dimensions for the amplification mechanism. If that is the case, the current Figure 1 would not be cited. Please correct.

Response: The concentration of Figure 1 (Protocol step 1.1) was incorrectly stated in the original manuscript. This has been rectified to "Construct an experimental platform including an improved 3D printer, a strain gauge indicator, a driving device, a support frame, an aluminum bar, a PDMS lens, a smartphone, weights, a printed amplifier, and a strain gauge, as shown in Figure 1".

3. Figure 2: 'Pringting' is a typo; please correct.

Response: We are apologize for the typo in Figure 2. It has been revised.

We greatly appreciate your help concerning improvement to this manuscript.

We have improved the manuscript and made the requested changes. The changes do not influence the results and conclusion of the study. The changes were marked in red in the revised document.

We hope that the corrections will satisfy your requests.

Thank you very much for your comments and suggestions.

Best regards,

Qiuyue Du

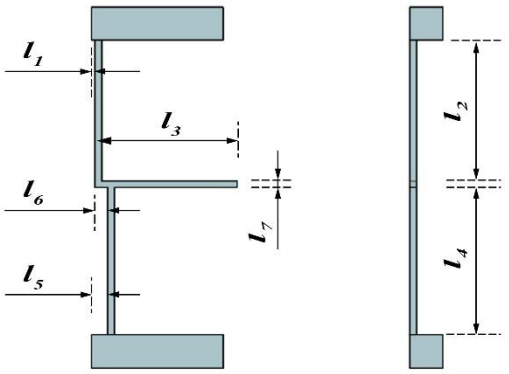


The length, width and height of the amplifying mechanism are 4×1×11mm, and the thickness of the upper and lower anchor pads is 1mm, and the thickness of the rest parts is 0.1mm.

Length: 4mm

Width: 1mm

Height: 11mm

Thickness of the upper and lower anchor pads: 1mm

Thickness of the rest parts: 0.1mm

$l_1$: 0.1mm

$l_2$: 4.5mm

$l_3$: 4mm

$l_4$: 4.5mm

$l_5$: 0.4mm

$l_6$: 0.3mm

$l_7$: 0.2mm